NUMERICAL CFD SIMULATION OF THE 1 MW_{TH} CFB CARBONATOR USING THE DISCRETE ELEMENT METHOD

Alexander Stroh*, **Martin Haaf, Alexander Daikeler, Maximilian von Bohnstein, Falah Alobaid, Jochen Ströhle, Bernd Epple**

Technische Universität Darmstadt, Institute for Energy Systems and Technology, Otto-Berndt-Straße 2, 64287 Darmstadt, Germany

*Email: *alexander.stroh@est.tu-darmstadt.de*

Abstract – A 1 MW_{th} pilot plant circulating fluidized bed (CFB) carbonator reactor is simulated under different operating conditions with the coarse grain discrete element method (DEM) in the context of the carbonate looping process. More specifically, the DEM is investigated in associations with the approach in which up to several thousands of particles are modelled by a representative single particle, so-called parcel. The simulation results under isothermal conditions are in good agreement with experimental measurements. For model validation, pressure transducer measurements along several reactor heights, gas concentrations and capacitive probe measurements (particle velocities and particle volume fractions) were used. Several particle size distributions were applied in the Lagrangian simulation to determine its influence on the numerical pressure profile. Furthermore, the DEM model is analyzed in terms of drag models by applying the Tang, Gidaspow, Wen and Yu, Syamlal O'Brien and Gibilaro models using custom-built User-Defined-Functions. The heterogeneous reaction between CaO and CO_2 is modelled according a reaction rate expression according (Hawthorne et al.). The reaction rate is crucially dependent on physical sorbent properties.

INTRODUCTION

Before the era of high performance computers, lab-scale experiments led to empirical approaches for calculating properties that are relevant in fluidized bed applications. Properties as for instance the minimum fluidization velocity, bubble formation rate, solids entrainment rate, gas-particle contact time scales, particle attrition or spatial solids distribution are of great importance in the design and operation of CFB units. Such lab-scale experiments (Adánez and Abanades 1991; Mathiesen et al. 2000) provided the basis for reactor design in commercial scale size applications. However experiments are environmentally unfriendly, also usually associated with costly measurements and high time expenditure. An alternative to experiments are numerical simulations that gained especially in the last decade particular importance in the prediction of gas-solid flows. The computational hardware performance further increased and numerical 3D simulations that are often referred as computational fluid dynamics (CFD) tools, moved into the center of attention. CFD tools allow to generate 3D simulation results within reasonable time and to use the results for studying reactor design modifications and complementing experimental data. It is worth to mention that many industrial applications include process time scales or microscopic phenomena that are still not feasible to be solved in CFD simulations because of not sufficient computational performance. Nonetheless, many large scale size applications are modeled with simplifications as it is demonstrated in the work by Odenthal et al. (Odenthal et al. 2006) who simulated a blast furnace taking into account a simplified interaction approach for the three Eulerian phases. Another particle related simplification in the discrete element method is the so called coarse grain approach in which many real sized particles are considered by one representative parcel (Sakai et al. 2014). By this simplification less particle trajectories are solved and consequently computational resources are saved. Despite all available simplifications, it is necessary to further develop CFD tools and validate proposed models with experimental data, not only for the sake of limited environmental resources but also due to increasing experimental costs. The objective of this work is the development and validation of a 3D model that represents a circulating fluidized bed (CFB) unit of 1 MW_{th} size in the calcium looping process. In this carbon capture and sequestration process, a mixture of calcium oxide (CaO) and calcium carbonate ($CaCO_3$) particles are circulating between two interconnected circulating fluidized bed reactors, carbonator and calciner respectively (Ströhle et al. 2014). The carbonator reactor is favorably operated at 650° C in order to account for optimum reaction atmospheres between CaO and CO_2 to $CaCO_3$ (Grasa et al. 2008).

EXPERIMENTAL BOUNDARY CONDITIONS

The carbonator reactor is 8.66 m in height and has an inner cross section diameter of 0.59 m (Figure 2). During the operation of the 1 MW_{th} pilot plant solid samples were continuously extracted at the reactor outlet,

reactor inlet (stream from calciner) and below the reactor nozzle bottom (screw conveyer). In total 154 hours operational hours were performed capturing CO_2 from a flue gas that originated from a coupled combustion chamber. During operation, the carbonator capture efficiency varied between 40-93% while the total plant CO_2 absorption efficiency was in the range of 70-96%. For model validation a 10 hour time span was selected in which the carbonate looping plant achieved stable operating conditions. The error for the overall mass balance between all streams entering and exiting the carbonator was approximately ~ 1 % which is in the magnitude of signal measurement standard deviations of used measurement apparatus. The collected samples were analyzed in terms of chemical composition and particle size distribution which are required for the proper definition of CFD boundary conditions. The particle size distribution (PSD) for the three extraction points is depicted in Figure 1.

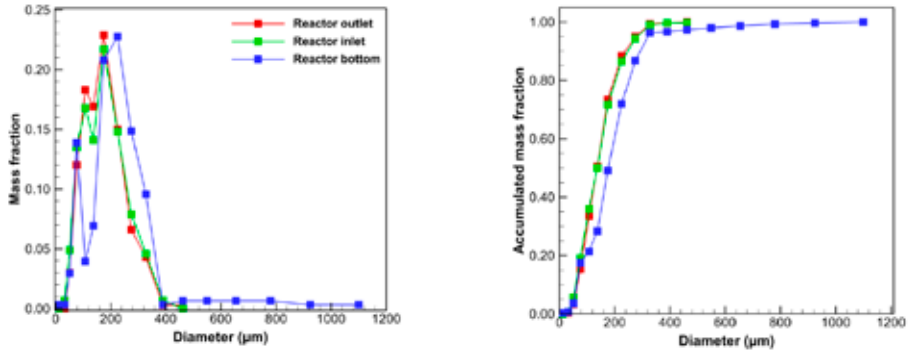

Figure 1: Particle size distribution at different extraction positions in the experiment

The PSD at the reactor inlet and outlet has a similar distribution while the PSD from the bottom of the reactor is shifted to bigger particle diameters.

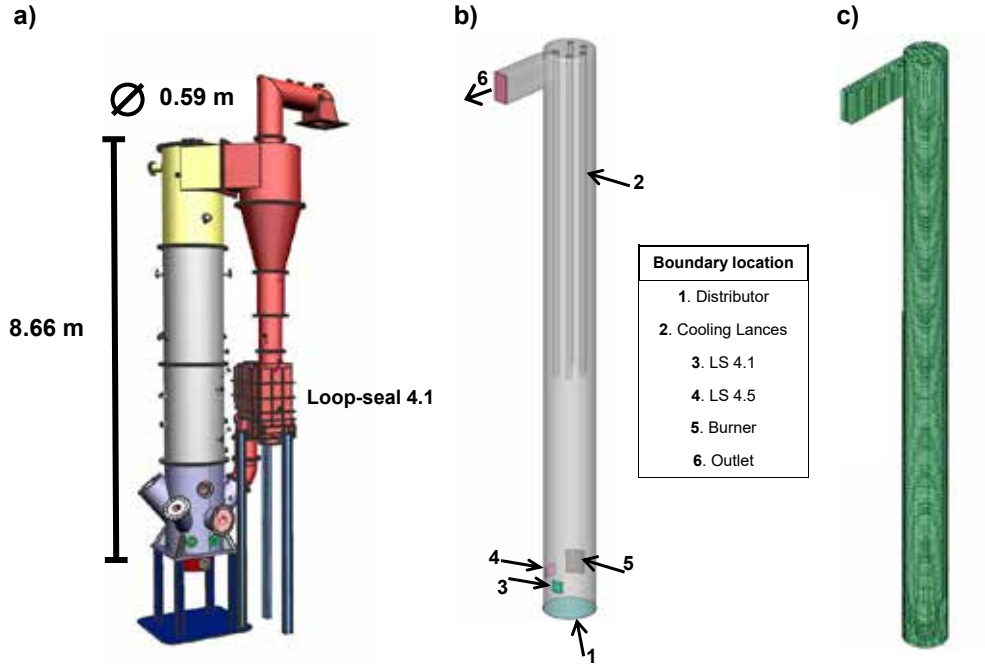

Figure 2: Carbonator reactor simplification a) CAD drawing of real sized model b) CFD geometry of riser only c) Discretization of the geometry

This fact can be attributed to the accumulation of coarser ash particles during long term pilot testing with pulverized hard coal. Besides gas concentrations at the outlet, pressure measurements, particle related measurements such as particle velocities and particle volume fractions were determined during plant operation (Daikeler et al. 2016). To the best knowledge of the authors, such a complete data set is rarely available in the literature for pilot plant sized CFB reactors and the validation work carried out is therefore very valuable for CFD model development. The Euler-Lagrange simulation was carried out using the PSD at the reactor outlet and the reactor bottom. Additionally to the simulations using PSD from the experiment, the mean Sauter diameter was used for a monodispersed parcel simulation. The derived gas composition and mass flow conditions from a closed energy and mass balance are summarized in Table 1. The reactor inventory was calculated from experimental pressure measurements to ~ 200 kg and the numerical temperature field was interpolated from experimental measurements along the reactor height.

Table 1: CFD mass flow and gas composition boundary data

Location	Temperature [°C]	Mass flow [kg/h]	Species mass fraction [%]	
Distributor (mf-inlet)	150	747	CO_2	0.201
			O_2	0.062
			H_2O	0.052
			N_2	0.685
Burner (mf-inlet)	35	103	O_2	0.233
			N_2	0.767
			Propane	0
LS4.5 (mf-inlet)	859	27	O_2	0.233
			N_2	0.767
		3693	CaO	0.829
			$CaCO_3$	0.004
			$CaSO_4$ + Ash	0.167
LS4.1 (mf-inlet)	615	33	O_2	0.233
			N_2	0.767
		UDF	Solid	100
Outlet (pressure outlet)	Temperature [° C]	Pressure [Pa]		
	602	0		

NUMERICAL MODEL

In this work the carbonator reactor is modeled and simulated in the ANSYS FLUENT™ software using the Lagrangian coarse grain discrete element method (parcels). The Euler-Lagrange model treats the fluid phase as a fluid and the particle phase as discrete elements. The fluid phase is solved based on the Navier-Stokes equations, while the particle movement is solved using Newtown's equation of motion. In this approach both parcel-fluid and parcel–parcel interactions are taken into account (Vreman et al. 2009). The mass conservation for each fluid phase is included by multiplying the continuity equation with the corresponding volume fraction of each phase as follows:

$$\frac{\partial}{\partial t}\left(\varepsilon_g \rho_g\right) + \nabla \cdot \left(\varepsilon_g \rho_g \vec{u}_g\right) = 0 \tag{1}$$

The momentum balance equation is extended by the volume fraction and the interaction term F_{DEM}, which couples the fluid phase with the corresponding solid phase. The fluid momentum equation can be written as:

$$\frac{\partial}{\partial t}\left(\varepsilon_g \rho_g \vec{u}_g\right) + \nabla \cdot \left(\varepsilon_g \rho_g \vec{u}_g \vec{u}_g\right) = -\varepsilon_g \nabla p + \nabla \cdot \left(\varepsilon_g \bar{\bar{\tau}}_g\right) + \varepsilon_g \rho_g \vec{g} + \vec{F}_{DEM} \tag{2}$$

The coupling term $\overrightarrow{F_{DEM}}$ considers the momentum change of all parcels located in one cell and is given as:

$$\vec{F}_{DEM} = \frac{\beta}{\varepsilon_g} \sum_{N_{Parcel}} \left(\vec{u}_p - \vec{u}_g\right) \tag{3}$$

The inter-phase exchange coefficient β can be calculated by using conventional drag models such as Syamlal O'Brien (Syamlal et al. 1993), Gidaspow (Gidaspow 1994) or a more sophisticated EMMS drag model (Qi et al. 2007). For instance, the inter-phase exchange coefficient of Wen and Yu (Wen and Yu 2013) drag model can be written as:

$$\beta_{Wen\&Yu} = \frac{3}{4}\frac{C_D \varepsilon_p \varepsilon_g \rho_g}{d_p}\left|\overrightarrow{u_p} - \overrightarrow{u_g}\right|\varepsilon_g^{-2.65} \quad (4)$$

Several other drag models are available in the literature to account for the momentum exchange between solid and fluid phase e.g. Gibilaro et al. (Gibilaro et al. 1985) or Tang et al. (Tang et al. 2015). The particle trajectory is computed based on the transitional motion equation:

$$\rho_p \frac{d\vec{u}_p}{dt} = \sum \vec{F}_p = \underbrace{\vec{F}_p}_{\text{volume force}} + \underbrace{\vec{F}_{drag}}_{\text{aerodynamic force}} + \underbrace{\vec{F}^n_{con} + \vec{F}^t_{con}}_{\text{contact Forces}} \quad (5)$$

The calculation of contact forces between two colliding parcels is schematically presented in Figure 3. The principle methodology is known as the soft-sphere approach in which two particles can overlap each other. Based on the overlapping magnitude a resulting contact force is computed using the Spring-Dashpot law. This law consists of a spring and a damper element with the damper term representing the energy dissipation during collision (Figure 3). Based on the spring constant and the overlap magnitude, the normal contact force is calculated. The dashpot term allows the modelling of inelastic collisions when using spring constant k and damping term γ. The normal force in newton is thus calculated (Fluent 2014) as:

$$\overrightarrow{F^n_{con,ı}} = \left(k\,\delta + \gamma\left(\vec{v}_{ij} \cdot \vec{n}_{ij}\right)\right)\vec{n}_{ij} \quad (6)$$

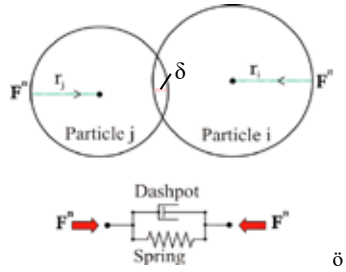

ö

Figure 3: Spring-Dashpot collision law

The tangential collisions forces are modelled by the friction collision law. This force is based on Coulomb friction:

$$\overrightarrow{F^t_{con}} = \mu\overrightarrow{F^n_{con}} \quad (7)$$

In Eq. (7) μ is the friction coefficient which depends on the relative velocity between particle and fluid phase. $\vec{F}^n_{con,i}$ represents the normal collision force and $\vec{F}^t_{con,i}$ the tangential force which is directed opposite to the relative tangential particle motion. The friction coefficient can be adjusted for different tangential velocities $|v_r|$ according to the description in the ANSYS FLUENT™ theory guide (Fluent 2014). The defined spring constant has a value of 500 N/m for Parcel-Parcel, Parcel-Wall interactions and fulfills the constrain for the particle time step size according Sullivan and Bray (O'Sullivan and Bray 2004). For the particulate matter resolution two types of parcels were used in the numerical model, namely multicomponent (CaO, $CaCO_3$, $CaSO_4$) reactive parcels and inert ash parcels that are not participating in any reaction with the fluid phase. The density of calcium carbonate was determined at the institute's laboratory. For pure calcium oxide the density is approximately ~ 1600 kg/m³, however due to high heating and cooling rates in the experiment a value of 1900 kg/m³ was estimated (Fischer 1955). For the calcium sulfate the same density as for calcium carbonate was assumed. For fly ash, a value of 1000 kg/m³ was used as it represents a broad range of coals (Epple et al. 2012). The initial mass composition of the multicomponent parcels was defined by the chemical composition at the reactor outlet, assuming ideal mixing in the CFB unit (Table 2). The fluid time step for the coupled CFD–DEM case is set to 1 millisecond while the particle time step is defined as 0.2 milliseconds. On the one hand lower particle time step sizes are required to properly resolve parcel-parcel and parcel-wall collisions. On the other hand the usage of higher particle time step sizes result in too large overlapping of parcels and lead to numerical instabilities. As concerns the spatial discretization of equations, for the coarse grain DEM simulation the second order QUICK scheme is applied for the solution

of the momentum and mass equations while for the time discretization a first order implicit scheme was used. Moreover, the phase-coupled SIMPLE algorithm is applied for the velocity-pressure coupling. For the accurate prediction of the pressure profile, the overall simulation time for each of the numerical simulations is approximately 20 seconds, with the last 15 seconds being used for time averaging.

Table 2: Particulate matter modelling and chemical composition data as boundary conditions

Parcel component	Density [kg/m³]	Initial mass fraction [%]
CaO	~ 1900	~ 80.0
$CaCO_3$	~ 2540	~ 9.5
$CaSO_4$	~ 2540	~ 10.5
Ash	~ 1000	

It was observed that 5 seconds after initialization, an equilibrium state is almost reached in every case. The Euler-Lagrange approach typically uses a numerical grid to discretize the equations of the continuous phase with the particles being tracked on the same grid. The average cell size in DEM simulations should be sufficiently small to capture small-scale structures of the fluid flow, however big enough to avoid numerical instabilities that are associated with a fully occupied cell by a single parcel. Nevertheless, the grid density is not the only parameter that affects the required resolution of the Euler-Lagrange models. Since particle numbers in industrial or even pilot plants are too high, the number of particles per parcel is a crucial parameter for the CFD model results accuracy (Li et al. 2012). According to this, two more resolution parameters for the DEM or MP-PIC parcel based simulations are currently proposed in the literature. The first resolution factor C_r denotes the average cell length to the parcel diameter and has a value of 3.02 in this work. The second resolution factor Pa_r represents the parcel to particle diameter and has a value of ~ 58 in this case. The applied mesh consists of ~ 100,000 hexahedral cells with a minimum orthogonal quality of 0.60 (Figure 2). In the beginning of the simulation the parcels were randomly placed in the numerical domain using an injection file that was created by a developed MATLAB code. The injection file contains 200,000 parcels with exact positions and zero initial velocities. The total mass of all parcels is ~ 200 kg. During the transient run, the number of injected parcels was controlled by User-Defined-Functions (UDF) in order to keep the inventory constant. The parcels were injected through the inlet port according experimental boundary condition. The focus lays on the correct prediction of the hydrodynamics and accurate gas concentrations along the carbonator height. The numerical results are compared to experimental measurements such as capacitive probe measurements (Daikeler et al. 2016), gas concentrations at the reactor outlet and several differential pressure signals over the reactor height. The reaction scheme according Charitos et al. (Charitos et al. 2010) and a proper drag resolution, that is important for the correct prediction of momentum exchange between fluid and solid phase, are realized by custom-built UDFs.

NUMERICAL RESULTS AND DISCUSSION

Figure 4 depicts the numerical results of time averaged pressure profiles along the reactor height in comparison with the experiment.

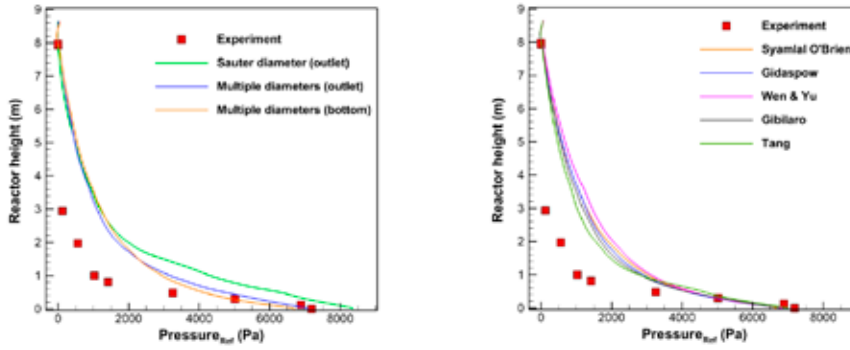

Figure 4: Pressure profiles left hand side: Influence of experimental PSD using Syamlal O'Brien drag model, right hand side: Influence of drag models using PSD at outlet

The numerical data on the left hand side was generated using the Syamlal O'Brien drag model. It can be clearly seen that the pressure profile is overpredicted for the mean Sauter diameter over the whole height of the reactor as well as for the multiple diameters simulation at heights above ~ 0.5 m using the same drag model. Generally a better fit to the experiment is achieved particularly at lower reactor heights when using multiple particle diameters for both PSDs. For the investigation of the drag model influence the upper mentioned drag models from the literature were used to simulate the 1 MW_{th} CFB unit. These drag models were developed based on theoretical and experimental studies for a certain range of conditions. A new drag correlation developed by Tang et al. (Tang et al. 2015) is derived from a computational study of fully resolved monodisperse static arrays of spheres for a broad range of particle Re numbers and solid volume fractions. This drag model quantitatively does not sufficiently match the experimental data above reactor heights of 0.5 m, however shows qualitatively very good agreement with the experiment. On one hand the time averaged pressure is homogenously distributed over the reactor cross section for all investigated drag models while on the other hand the time averaged particle distribution is inhomogeneous and higher concentrated in the vicinity of reactor walls. Especially the solids volume fraction close to the inlet port is increased (Figure 5).

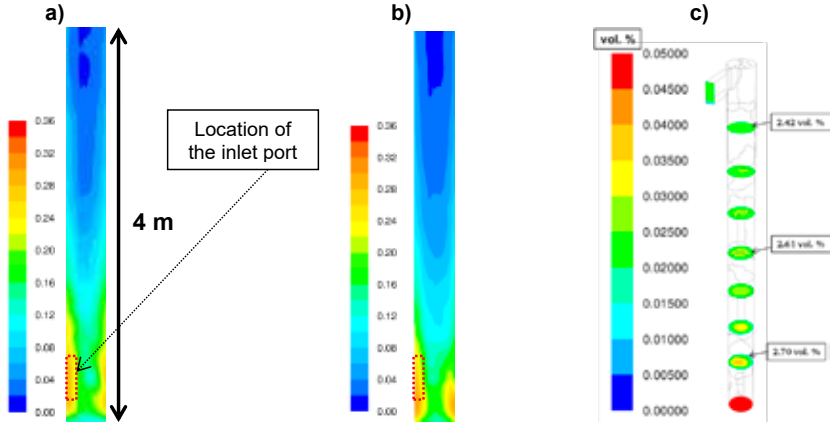

Figure 5: Comparison of time averaged particle volume fraction using (a) Syamlal O'Brien (b) Tang et al. drag model; (c) Time averaged CO_2 concentration inside the reactor using Syamlal O'Brien drag model

Generally a typical core annular flow pattern can be observed in the contour plots. The simulated solid volume fraction is overpredicted by a factor of ~ 10 at a reactor height of 4.4 m is a result of an overpredicted drag force. Drag models based on the energy minimization theory (Li et al. 2012; Stroh et al. 2015; Zeneli et al. 2015) are capable to predict the pressure profile more accurate.

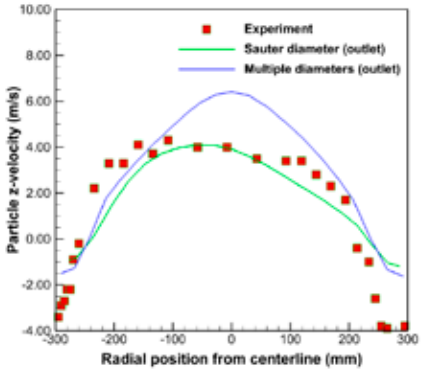

Figure 6: Time averaged parcel velocities using Syamlal O'Brien drag model in comparison with the experiment

However such models require the solution of a minimization problem including 6 or more variables depending on the model boundaries. Generally such an approach is computationally too expensive to be implemented in a transient particle simulation, hence needs a pre-calculation of drag correction terms outside the CFD software. When comparing the particle z-velocities at a reactor height of 4.4 m with capacitive probe measurements (Daikeler et al. 2016) the velocity agreement is good for the representative Sauter diameter, especially in the reactor center. For the multiple diameters simulation the velocities in the center are overpredicted due to mainly smaller particles that were entrained with the flow. In the vicinity of walls, both numerical cases underestimate particle backflow velocities. The carbonation reaction rate depends on several experimental parameters such as gas composition, make-up mass flow rate, physical sorbent properties and

CO_2 equilibrium concentration (Donat et al. 2012). For simplicity reasons the numerical temperature field was linearized by using experimental temperature measurements along the reactor height. The investigation of the CO_2 profile along the reactor height and reactor cross section confirmed the typical core annular flow (Figure 5). The time averaged mean CO_2 outlet concentrations deviates approximately 6 % from the experimental value. This is a very good result considering the complexity of the boundary conditions and the carbonation reaction.

CONCLUSION

In this work a pilot plant 1 MW_{th} CFB carbonator unit was simulated with the coarse grain DEM model using experimental boundary conditions of a calcium looping process during long-term stable operation. The coarse grain DEM model was investigated in a parametric study varying the resolution factors C_r (average cell length to the parcel diameter) and Pa_r (parcel diameter to particle diameter). A value of 3.02 for C_r showed an independent result for the computed pressure profile while a value of 58 for Pa_r was sufficiently small to have no further influence on the simulation results. Several interesting findings on the hydrodynamics of the CFB unit could be determined numerically: Firstly, the influence on the pressure profile of applied particle size distributions from different extraction locations in the experiment was elaborated. Both PSD samples yield a similar numerical pressure profile even though one sample had not negligible bigger diameters. Secondly, the Sauter mean diameter that is often used in numerical studies, showed an overprediction of the pressure profile along the whole reactor height. Thirdly, the coarse grain DEM model is analyzed in terms of momentum exchange between solid and fluid phase by applying the Tang, Gidaspow, Wen and Yu, Syamlal O'Brien and Gibilaro drag models using custom-built UDFs in the numerical model. The numerical pressure profile showed for all models qualitatively a good agreement with experimental data however all models quantitatively overpredicted the pressure profile above a reactor height of ~ 0.5 m. The computed particle velocities are in good agreement with experimental measurements at a rector height of 4.4 m using the Sauter mean diameter. For the multiple particle diameters simulations the central particle velocities were numerically overpredicted while the backflow particle velocities in the vicinity of walls underpredicted. The solids volume fraction and as well the CO_2 concentration confirmed the typical core annulus flow in the cfb unit. The heterogeneous reaction between CaO and CO_2 is modelled according available a reaction rate expression from the literature (Charitos et al. 2010). The time averaged CO_2 reactor concentration correlated well with the solids distribution. The CO_2 volume concentration was increased in the reactor center where less reactive particles are located. The reactor outlet CO_2 vol. % concentration deviated approximately by 6 % from experimental data. In future investigations the drag model by Tang et al. will be corrected based on an in-depth examination of the friction coefficient and solids volume fraction in the numerical domain.

NOTATION

Roman symbols

d	Diameter, [m]	C_r	Average cell length to parcel diameter ratio
g	Gravitational acceleration, [m/s²]	F	Force, [N/kg]
u	Velocity, [m/s]	Pa_r	Parcel diameter to particle diameter ratio
$v_{r,p}$	Terminal velocity correlation, [m/s]		
C_D	Dimensionless drag coefficient, [-]		

Greek Symbols

β	Fluid-solid exchange coefficient, [kg/(m³s)]	ε	Volume fraction, [-]
γ	Damping coefficient in DEM model, [-]	μ	Friction coefficient, [-]
δ	Overlapping magnitude in DEM model, [m]	μ_g	Gas shear viscosity, [kg/(m²s)]
		ρ	Density, [kg/m³]
		$\bar{\bar{\tau}}_g$	Stress-strain tensor, [Pa]

Subscripts

con	Contact between colliding partners	g	Gas
		p	Particle/Parcel
DEM	Coupling term for momentum exchange between particle and		fluid phase

REFERENCES

Adánez, J. & Abanades, J. 1991. Minimum fluidization velocities of fluidized-bed coal-combustion solids. *Powder Technology*, **67**, 113-119.

Charitos, A., Hawthorne, C., Bidwe, A., Sivalingam, S., Schuster, A., Spliethoff, H. & Scheffknecht, G. 2010. Parametric investigation of the calcium looping process for CO 2 capture in a 10kW th dual fluidized bed. *International Journal of Greenhouse Gas Control*, **4**, 776-784.

Daikeler, A., Ströhle, J. & Epple, B. 2016. Experimentelle Untersuchung der lokalen Strömungsverhältnisse in einer 1 MWth Wirbelschichtanlage mittels eines kapazitiven Messsystems. *Jahrestreffen der ProcessNet-Fachgruppen Agglomerations- und Schüttguttechnik, Mehrphasenströmungen und Computational Fluid Dynamics*, Bingen am Rhein.

Donat, F., Florin, N.H., Anthony, E.J. & Fennell, P.S. 2012. Influence of high-temperature steam on the reactivity of CaO sorbent for CO2 capture. *Environmental Science & Technology*, **46**, 1262-1269.

Epple, B., Leithner, R., Linzer, W. & Walter, H. 2012. Simulation von Kraftwerken und Feuerungen. Springer-Verlag.

Fischer, H. 1955. Calcination of Calcite: I, Effect of Heating Rate and Temperature on Bulk Density of Calcium Oxide. *Journal of the American Ceramic Society*, **38**, 245-251.

Fluent. 2014. Theory Guide.

Gibilaro, L., Di Felice, R., Waldram, S. & Foscolo, P. 1985. Generalized friction factor and drag coefficient correlations for fluid-particle interactions. *Chemical Engineering Science*, **40**, 1817-1823.

Gidaspow, D. 1994. Multiphase flow and fluidization: continuum and kinetic theory descriptions. Academic press.

Grasa, G.S., Abanades, J.C., Alonso, M. & González, B. 2008. Reactivity of highly cycled particles of CaO in a carbonation/calcination loop. *Chemical Engineering Journal*, **137**, 561-567.

Hawthorne, C., Charitos, A., Perez-Pulido, C., Bing, Z. & Scheffknecht, G. Design of a dual fluidised bed system for the post-combustion removal of CO2 using CaO. Part I: CFB carbonator reactor model.

Li, F., Song, F., Benyahia, S., Wang, W. & Li, J. 2012. MP-PIC simulation of CFB riser with EMMS-based drag model. *Chemical Engineering Science*, **82**, 104-113.

Mathiesen, V., Solberg, T. & Hjertager, B.r.H. 2000. An experimental and computational study of multiphase flow behavior in a circulating fluidized bed. *International Journal of Multiphase Flow*, **26**, 387-419.

O'Sullivan, C. & Bray, J.D. 2004. Selecting a suitable time step for discrete element simulations that use the central difference time integration scheme. *Engineering Computations*, **21**, 278-303.

Odenthal, H.-J., Falkenreck, U. & Schlüter, J. 2006. CFD simulation of multiphase melt flows in steelmaking converters. *ECCOMAS CFD 2006: Proceedings of the European Conference on Computational Fluid Dynamics, Egmond aan Zee, The Netherlands, September 5-8, 2006*. Delft University of Technology; European Community on Computational Methods in Applied Sciences (ECCOMAS).

Qi, H., Li, F., Xi, B. & You, C. 2007. Modeling of drag with the Eulerian approach and EMMS theory for heterogeneous dense gas–solid two-phase flow. *Chemical Engineering Science*, **62**, 1670-1681.

Sakai, M., Abe, M., Shigeto, Y., Mizutani, S., Takahashi, H., Viré, A., Percival, J.R., Xiang, J. & Pain, C.C. 2014. Verification and validation of a coarse grain model of the DEM in a bubbling fluidized bed. *Chemical Engineering Journal*, **244**, 33-43.

Stroh, A., Ströhle, J. & Epple, B. 2015. CFD simulation of 1 MW Carbonator. *http://www.ieaghg.org/docs/General_Docs/6_Sol_Looping/4_AlexanderStroh_MilanSEC.pdf*.

Ströhle, J., Junk, M., Kremer, J., Galloy, A. & Epple, B. 2014. Carbonate looping experiments in a 1MWth pilot plant and model validation. *Fuel*, **127**, 13–22, doi: 10.1016/j.fuel.2013.12.043.

Syamlal, M., Rogers, W. & O'Brien, T.J. 1993. MFIX documentation: Theory guide. *National Energy Technology Laboratory, Department of Energy, Technical Note DOE/METC-95/1013 and NTIS/DE95000031*.

Tang, Y., Peters, E., Kuipers, J., Kriebitzsch, S. & Hoef, M. 2015. A new drag correlation from fully resolved simulations of flow past monodisperse static arrays of spheres. *AIChE Journal*, **61**, 688-698.

Vreman, B., Geurts, B., Deen, N.G., Kuipers, J.A.M. & Kuerten, J.G.M. 2009. Two- and Four-Way Coupled Euler–Lagrangian Large-Eddy Simulation of Turbulent Particle-Laden Channel Flow. *Flow, Turbulence and Combustion*, **82**, 47-71, doi: 10.1007/s10494-008-9173-z.

Wen, C. & Yu, Y. 2013. Mechanics of fluidization. *Chem. Eng. Prog. Symp. Ser.*, 100.

Zeneli, M., Nikolopoulos, A., Nikolopoulos, N., Grammelis, P. & Kakaras, E. 2015. Application of an advanced coupled EMMS-TFM model to a pilot scale CFB carbonator. *Chemical Engineering Science*, **138**, 482-498.